

G_2 gauge theory at finite temperature

Guido Cossu

*Scuola Normale Superiore, Piazza dei Cavalieri 27, 56126 Pisa
and INFN Pisa, Largo B. Contecorvo 3 Ed. C, 56127 Pisa, Italy
E-mail: g.cossu@sns.it*

Massimo D'Elia

*Dipartimento di Fisica & INFN Genova, Via Dodecaneso 33, 16146 Genova, Italy
E-mail: delia@ge.infn.it*

Adriano Di Giacomo

*Dipartimento di Fisica & INFN Pisa, Largo B. Contecorvo 3 Ed. C, 56127 Pisa, Italy
E-mail: adriano.digiacomio@df.unipi.it*

Biagio Lucini

*Department of Physics, Swansea University, Singleton Park, Swansea SA2 8PP, UK
E-mail: b.lucini@swansea.ac.uk*

Claudio Pica

*Physics Department, Brookhaven National Laboratory, Upton, NY 11973, USA
E-mail: pica@bnl.gov*

ABSTRACT: The gauge group being centreless, G_2 gauge theory is a good laboratory for studying the role of the centre of the group for colour confinement in Yang-Mills gauge theories. In this paper, we investigate G_2 pure gauge theory at finite temperature on the lattice. By studying the finite size scaling of the plaquette, the Polyakov loop and their susceptibilities, we show that a deconfinement phase transition takes place. The analysis of the pseudocritical exponents give strong evidence of the deconfinement transition being first order. Implications of our findings for scenarios of colour confinement are discussed.

KEYWORDS: Lattice Gauge Field Theories, Confinement.

Contents

1. Introduction	1
2. Basic properties of the exceptional group G_2	3
3. Simulations of G_2 Lattice Gauge Theory	4
4. Thermodynamics of G_2 gauge theory	6
5. Discussion	9
6. Conclusions	10
A. G_2 algebra representation	11
B. Algebra	11

1. Introduction

Confinement is one of the most elusive problems in QCD. There is strong experimental evidence that quarks and gluons, which are the fundamental degrees of freedom of the theory, never appear as final states of strong interactions. It is still a challenge to understand how confinement is encoded in the QCD Lagrangian.

Following the large number of colours idea [1], it is reasonable to conjecture that confinement is a property of the gauge sector of the theory. Hence, it should be possible to solve the problem by looking at the pure gauge theory, and the solution should not be specific to a given number of colours N . For the pure gauge theory at finite temperature, it has been shown that confinement is lost at some critical temperature T_c [2]. The deconfinement phase transition in $SU(N)$ gauge theories can be understood in terms of the centre of the gauge group, which is \mathbb{Z}_N . An order parameter for the phase transition is the Polyakov loop

$$L(\vec{x}, T) = \frac{1}{n} \text{Tr} \exp \left(ig \int_0^{1/T} A_0 dt \right) , \quad (1.1)$$

where A_0 is the gauge field in the compact direction, naturally associated to the temperature T , whose length is $1/T$, g is the gauge coupling and n the dimension of the fundamental representation (in $SU(N)$, $n = N$). Since one dimension is compact, gauge transformations which are continuous modulo $2\pi/g$ are acceptable in the theory. Under those transformations, $L(\vec{x}, T) \rightarrow zL(\vec{x}, T)$, where z is an element of \mathbb{Z}_N . If the centre symmetry is not broken, $\langle L \rangle = (1/V) \int L(\vec{x}, T) d^3x = 0$ in the thermodynamic limit $V \rightarrow \infty$, V being the

volume of the system. Conversely, a value of $\langle L \rangle$ different from zero implies breaking of the centre symmetry. It is possible to show that at low temperatures $\langle L \rangle = 0$, while at high temperatures $\langle L \rangle \neq 0$. Hence, a centre symmetry breaking phase transition must take place. The expectation value of the Polyakov loop can be related to the free energy F of a static quark as

$$L \propto e^{-\beta F} . \quad (1.2)$$

It is then natural to identify the centre symmetry breaking phase transition with the deconfinement phase transition. In a famous paper [3], Svetitsky and Yaffe conjectured that the universality class of the deconfinement phase transition for $SU(N)$ gauge theory in $D=d+1$ dimensions is that of a d -dimensional \mathbb{Z}_N Potts model, provided that the latter has a second order phase transition. The Svetitsky-Yaffe conjecture has been verified numerically in $3+1$ and $2+1$ dimensions (see [4, 5] for recent lattice calculations). It is interesting to remark that whenever the underlying spin model has a first order phase transition, so does the $SU(N)$ gauge theory.

This analysis hints toward the relevance of the centre for confinement. An independent way to relate centre symmetry and confinement is presented in [6], where confinement is described in terms of condensation of vortices carrying magnetic flux. The allowed N magnetic fluxes are in one to one correspondence with the centre elements of the group. Condensation of vortices in the confined phase means that the area spanned by a Wilson loop randomly intersect vortex worldsheets. The resulting cancelations determine the so-called area law for the Wilson loop, which is one of the accepted criteria for colour confinement. Numerical works have confirmed the vortex scenario [7]. To characterise the transition in terms of a symmetry, the 't Hooft loop operator can be introduced [6], which is expected to have a non-zero vacuum expectation value in the confined phase and to be zero in average in the deconfined phase. This behaviour has been checked numerically in [8, 9, 10, 11].

While this scenario for colour confinement is perfectly consistent, the centre symmetry is lost when dynamical fermions are added to the action. Hence, either one gives up the idea that confinement in the pure Yang-Mills theory and in the full theory is basically the same phenomenon or we must assume that the centre is just a useful way to look at confinement, but does not embody any fundamental physics in relation to it. One possible way to look at this issue is to study the deconfinement phase transition in other gauge groups that have a different centre pattern. The physics of the phenomenon being inherently non-perturbative, lattice calculations are well suited for those investigations. In this context, $SO(3) \equiv SU(2)/\mathbb{Z}_2$ would be an ideal candidate: it is expected to confine (like $SU(2)$, since the two groups share the same algebra), but has a trivial centre. Recent results suggest that a deconfinement phase transition takes place, but the presence of lattice artifacts (*centre monopoles*) makes it difficult to extract a reliable continuum limit [12]. Moreover, the centre structure of the underlying universal covering group ($SU(2)$) reflects in the existence of twist sectors, which might imply that the centre still plays a role, despite the group being centreless.

A different way to approach the problem is to use a fundamental group that is genuinely

centreless¹. The simplest group in this category is the exceptional group G_2 . There are other properties that make G_2 interesting for QCD: it contains $SU(3)$ as a subgroup and (as in full QCD) an asymptotic string tension does not exist, since the colour charge carried by a quark can be completely screened by gluons [13]. The existence of two phases has been proved in [13]. However, this does not exclude that, instead of a real phase transition, a crossover separates the two phases. Were this the case, the physics of deconfinement in G_2 would be noticeably different from that of $SU(N)$ gauge theories, and this would cast serious doubts about what we can learn from G_2 for confinement in more physical gauge theories. While data reported in [14, 15] are compatible with a first order phase transition taking place, no exhaustive and detailed study of deconfinement has been performed so far. In this paper, we shall fill this gap by studying the finite size scaling behaviour of the plaquette, of the Polyakov loop and of their susceptibilities, from which we extract the critical exponents for the transition. We will then be able to show that a real transition takes place and that this transition is first order.

This work is organised as follows. In Sect. 2 we will review the basic properties of the exceptional group G_2 . Details of our lattice simulations are presented in Sect. 3. Sect. 4 contains our results and provides evidence for a first order deconfinement phase transitions occurring in G_2 at finite temperature. The implications of our findings for possible mechanisms of colour confinement are discussed in Sect. 5. Finally, in Sect. 6 we summarise the main points of our investigation.

2. Basic properties of the exceptional group G_2

We begin by summarising some basic properties of the Lie Group G_2 . In mathematical terms this is the group of automorphisms of the octonions and it can be naturally constructed as a subgroup of the real group $SO(7)$ - which has 21 generators and rank 3. Besides the usual properties of $SO(7)$ matrices

$$\det \Omega = 1 \quad \Omega^{-1} = \Omega^T \quad (2.1)$$

we have in addition another constraint

$$T_{abc} = T_{def} \Omega_{da} \Omega_{eb} \Omega_{fc} \quad (2.2)$$

where T_{abc} is a totally antisymmetric tensor whose nonzero elements are (using the octonion basis given by [16])

$$T_{123} = T_{176} = T_{145} = T_{257} = T_{246} = T_{347} = T_{365} = 1. \quad (2.3)$$

Equations (2.2) are 7 independent relations reducing the numbers of generators to 14. The fundamental representation of G_2 is 7 dimensional. Using the algebra representation of [16] (we refer to appendix A for details) we can clearly identify an $SU(3)$ subgroup and several $SU(2)$ subgroups, 6 of which are sufficient to cover the whole group, a useful property for

¹We use the word centreless to refer to a group whose centre is given only by the unity element.

MC simulations. The first three $SU(2)$ subgroups are in the 4×4 real representation of the group while the remaining three are a mixture of the 4×4 and the 3×3 representations and are extremely difficult to simulate with standard heat-bath techniques. See the next section for details on simulations.

The following relations hold:

$$SU(3) \subset G_2 \Rightarrow \mathcal{C}(G_2) \subset \text{Centr}(SU(3)) = \mathbb{Z}_3 \quad (2.4)$$

in which $\text{Centr}(SU(3))$ is the centralizer of $SU(3)$ (i.e. the matrices in G_2 that commute with every element in $SU(3)$). Intersections of centralizers of different $SU(3)$ subgroups give

$$\mathcal{C}(G_2) = \{1\} \quad (2.5)$$

i.e. a trivial centre.

The Lie group G_2 has rank 2, like $SU(3)$. This implies that the residual symmetry after an Abelian projection is $U(1)^2$, its Cartan subgroup. Stable monopole solutions are classified according to the homotopy group²:

$$\pi_2(G_2/U(1)^2) = \pi_1(U(1) \times U(1)) = \mathbb{Z} \times \mathbb{Z} \quad (2.6)$$

i.e. we have two distinct species of monopoles, classified by elements of the discrete group \mathbb{Z}_2 , as for $SU(3)$. An extension of the 't Hooft tensor - the gauge invariant field of monopoles - can be written for the G_2 gauge group so Abelian monopole solutions are really possible in this theory.

Another interesting homotopy group shows that centre vortices are absent in the theory:

$$\pi_1(G_2/\mathcal{C}(G_2)) = \pi_1(G_2) = 0 \quad (2.7)$$

while for $SU(3)$ for example

$$\pi_1(SU(3)/\mathbb{Z}_3) = \mathbb{Z}_3 \quad (2.8)$$

and

$$\pi_1(SO(3)/\{1\}) = \pi_1(SO(3)) = \mathbb{Z}_2 \neq 0 \quad (2.9)$$

as stated before. So G_2 is a good playground to study the dual superconductor picture in a theory without centre vortices, thus isolating monopole contribution in confinement.

3. Simulations of G_2 Lattice Gauge Theory

In this work we are going to investigate the thermodynamical properties of the gauge group G_2 (see also [13, 14]). To simulate the pure gauge theory

$$\mathcal{L} = \frac{1}{7g^2} \text{Tr} F_{\mu\nu} F_{\mu\nu} \quad (3.1)$$

²The first equality follows from $\pi_1(G_2) = 0$. See for example [17].

with the Wilson action, we used a simple Cabibbo-Marinari update (heat-bath + overrelaxation in a tunable ratio, for every step) for the first three $SU(2)$ subgroups (4×4 representation, set 1,3 and 4 in appendix A) spanning the $SU(3) \subset G_2$. This simple setting cannot be used for the remaining three subgroups because the integration measure is not as simple. We make a random gauge transformation every n updates (typically 1 or 2) to guarantee the ergodicity of the algorithm³. To study the thermodynamical properties we simulated several asymmetric lattices $N_t \times N_s^3$ of spatial dimensions $N_s = 12, 14, 16, 18, 20, 24, 32$ and temporal dimension $N_t = 6$ ($N_t = 4$ only for the smallest lattice). An average of 20 β s per lattice have been simulated. The temperature of the system is given by $T = (a(\beta)N_t)^{-1}$, where $a(\beta)$ is the lattice spacing as a function of $\beta = 1/7g^2$. The critical behaviour of the system has been extracted by applying the theory of finite size scaling (FSS), which has been used to extrapolate the behaviour of the observables we have studied to the thermodynamic limit ($N_s \rightarrow \infty$). We needed histories of order 10^5 updates near the transition (1 week on a 1.5GHz Opteron processor for a medium lattice).

The code is highly optimized and very fast (using only real algebra), is written using explicitly assembler SSE2 instructions in single precision for the matrix-multiplication core and run on an Opteron farm in the computer facilities of the Physics Department of the University of Pisa.

The observables we have measured are the standard plaquette and the Polyakov loop. A clarification is in order here. While one should expect to be able to characterise the critical behaviour of a system by looking at the plaquette, doubts could be cast into the usefulness of the Polyakov loop: since G_2 is centreless, the Polyakov loop is not an order parameter for a possible deconfining phase transition. In principle, phase transitions can be reliably investigated only by using an order parameter field, whose critical behaviour characterises the transition itself. However, in order to prove that a transition takes place and to determine the critical indices, a non-trivial overlap on the order parameter is the only property we need⁴. Hence, if we can observe a divergence in the peak of the Polyakov loop susceptibility (and of the specific heat, whose reliability is hard to question) we can safely conclude that a phase transition takes place.

The theory of FSS predicts that as a function of the volume the maximum of susceptibilities scale in the following way:

$$\chi \sim a \cdot L^{\frac{\gamma}{\nu}} + b, \quad (3.2)$$

where γ is the critical exponent of the generating quantity (in our case either the plaquette or the Polyakov loop) and ν is the critical exponent related to the divergence of the correlation length. The position of the maximum scales as

$$\beta_c(L) = \beta_c(\infty) + cL^{-1/\nu}, \quad (3.3)$$

where $\beta_c(L)$ is the pseudocritical β for size L and $\beta_c(\infty)$ is the critical value of β . This analysis also applies to first order phase transition, whose signature is given by $\gamma = 1$ and

³The matrices for random gauge transformation are regenerated every step by a random algorithm to assure that no periodicities or orbits in phase space can arise.

⁴The reverse of this sentence is not true: no conclusion can be drawn from the absense of critical behaviour in a non-order parameter field.

$\nu = 1/d$, with d the dimension of the system.

4. Thermodynamics of G_2 gauge theory

We studied the thermodynamics of this theory using the typical observables, the plaquettes

$$P_s = \frac{1}{3 \cdot 7 N_s^3 N_t} \sum_{\square_s} \text{Tr} U_{\square_s} \quad P_t = \frac{1}{3 \cdot 7 N_s^3 N_t} \sum_{\square_t} \text{Tr} U_{\square_t} \quad (4.1)$$

where the two sums are on space-space and space-time plaquettes respectively. The peak of the susceptibility

$$\chi_P = N_s^3 (\langle P^2 \rangle - \langle P \rangle^2) \quad P = (P_s + P_t)/2 \quad (4.2)$$

signals the phase transition point. This quantity (often referred to in the literature as the "lattice specific heat") is only part of the (physical) specific heat, whose complete reconstruction requires various correlators weighted with different coefficients; nonetheless, this is a singular piece from which the critical scaling behaviour can be inferred.

We also measured the Polyakov loop and its susceptibility:

$$L = \frac{1}{N_s^3} \sum_{\vec{x}} \left(\frac{1}{7} \prod_{t=0}^{N_t-1} U_4(\vec{x}) \right) \quad \chi_L = N_s^3 (\langle L^2 \rangle - \langle L \rangle^2). \quad (4.3)$$

The lattices considered for the scaling analysis are only the $N_s = 12, 14, 16, 18, 20$ times $N_t = 6$ for the following reasons. The computational cost of locating the transition grows exponentially fast with the volume; anticipating here a first order transition, the intrinsic problem is that two (or more) phases coexist. The simulated system tunnels between pure phases by building an interface of size N_s . The free-energy cost of such a mixed configuration is σN_s^{D-1} (σ being the surface tension), the interface is built with probability $\exp(-\sigma N_s^{D-1})$ and the natural time scale for the simulation grows with N_s as $\exp(\sigma N_s^{D-1})$. This is called exponential critical slowing down and makes simulations impractical for lattices with $N_s > 20$ for a reliable estimate of susceptibilities. Looking at Figs. 4, 5 and comparing the densities in the tunneling region for the three different lattices gives an idea of the problem, common to all systems exhibiting a first order transition. Multicanonical methods [18] will be needed for feasible simulations on such large lattices. The other reason concerns the number of time slices and is related to the presence of an unphysical bulk transition that we shall explain below (see also Fig. 1). Being very close to the bulk transition, the physical deconfinement transition for $N_t = 4$ is extremely difficult to detect, the signal being highly contaminated by the "noise" coming from the bulk. $N_t = 6$ is needed to be sufficiently away from the bulk. By increasing furtherly N_t , one can move the physical transition far away from the bulk transition point. Hence, choosing a larger N_t will clean the signal from the bulk "noise". To investigate this possibility, we performed some simulations at $N_t = 8$, which confirmed the general features of the $N_t = 6$ simulation. The displacement of the critical β was clearly visible but not sufficient to bring any practical

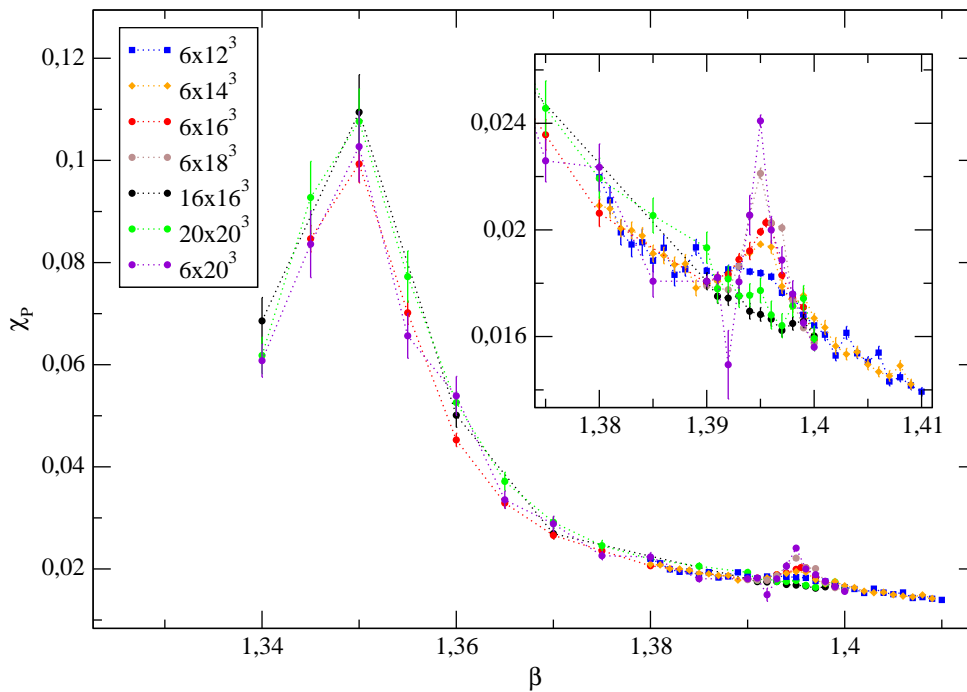


Figure 1: Plaquette susceptibility plotted against β . The peak signals the bulk transition while the peak corresponding to the physical transition for $N_t = 6$ is shown in the inset. We also show results from a simulation at $T=0$ on a 16^4 lattice (black triangle points).

advantage over the $N_t = 6$ calculation, while the simulation time increased considerably. For this reason, we stuck to the $N_t = 6$ calculation, giving up the possibility of performing a continuous limit extrapolation of the critical temperature. However, our pilot study at $N_t = 8$ suggests that there is no reason to doubt that such a continuous limit exists.

In a finite volume no divergences can arise, since the partition function is analytical. Nevertheless critical indices can be measured by looking at the scaling with the volume of the plaquette susceptibility (related to the specific heat C_V). The height of the peak for a first-order transition scales with the volume V and the width and the displacement from the real critical point of the peak position scales as $1/V$ (plus corrections to this leading behaviour).

A pronounced peak is present at any volume and N_t and always at the same $\beta \sim 1.35$. There is no scaling with volume and no movement toward the weak coupling region passing from $N_t = 4$ to $N_t = 6$ as we would expect for a physical transition. This transition is the equivalent of the bulk phase transition in $SU(N)$ gauge theories, and separates the (physical) weak coupling region from the (unphysical) strong coupling one. The bulk peak almost completely overshadows the real physical transition, a smaller peak in the weak coupling region at $\beta \sim 1.395$ for $N_t = 6$. This peak scales with the volume, provided that the bulk contribution has been subtracted. This subtraction procedure is needed in order to disentangle the physics from the discretisation artifacts. To estimate the bulk background, we simulated the system also at zero temperature on 16^4 and 20^4 lattices (to control systematic errors). The bulk contribution has to be subtracted from the plaque-

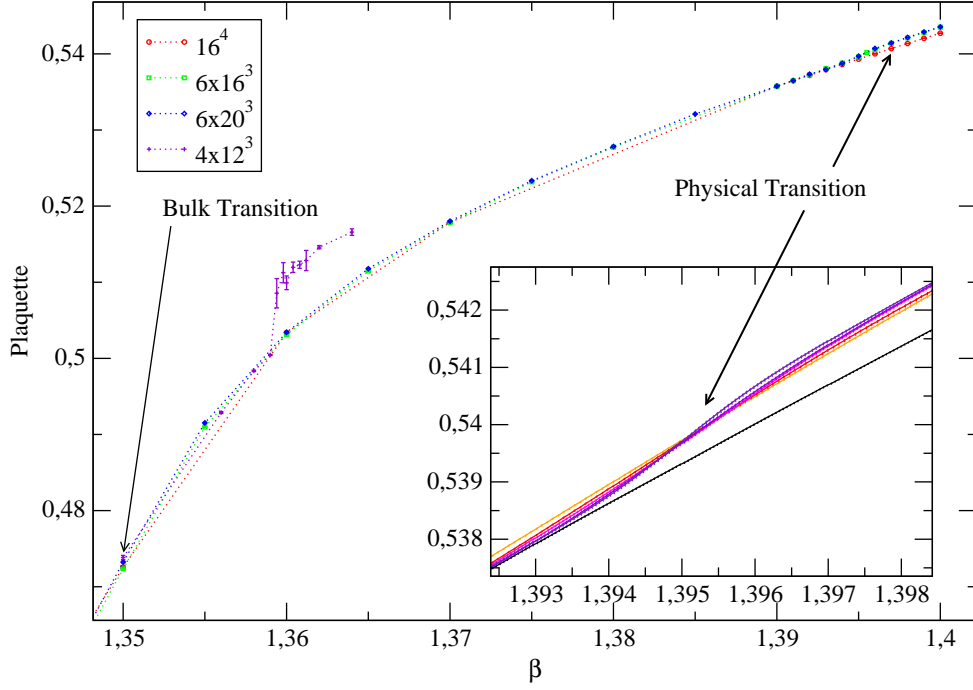


Figure 2: Comparison of finite and zero temperature simulations. In the box: magnification of the physical transition region (reweighted curves).

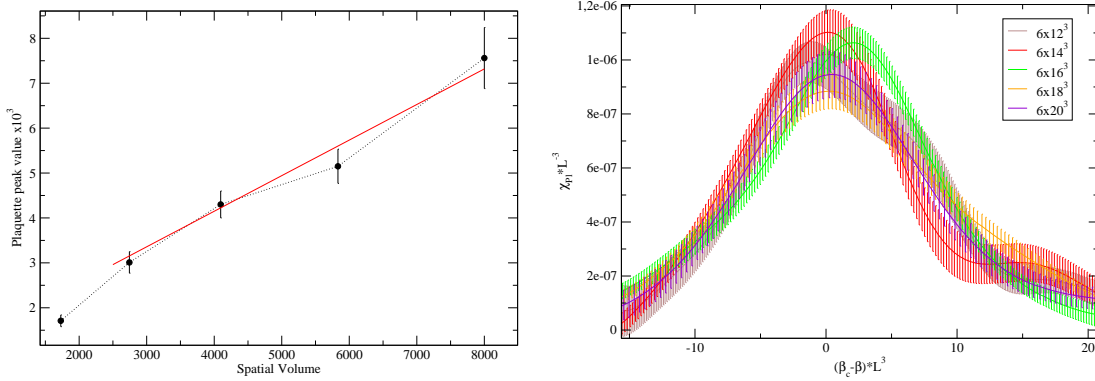


Figure 3: Left: scaling of the peak of plaquette susceptibility with the volume. The continuous line is a linear fit to the data, as explained in the text. Right: FSS of the plaquette susceptibility assuming a first order transition. For this plot, we have used the value $\beta_c = 1.395$, obtained from the fit to the position of the maximum according to (3.3).

the susceptibility for a correct finite scaling analysis. This procedure could be seen as a normalisation of the free energy following the request that this quantity be zero at zero temperature. The influence of the bulk transition on the plaquette susceptibility is shown in Fig. 1. The nature of the two transitions manifests itself comparing finite temperature and zero temperature simulations in Fig. 2. The integral of the difference between the two

curves is the free energy density:

$$\left. \frac{f}{T^4} \right|_{\beta_0}^{\beta} = -N_{\tau}^4 \int_{\beta_0}^{\beta} d\beta' (P_0 - P_T) \quad (4.4)$$

in which P_0 and P_T are the mean plaquettes at zero and finite temperature respectively. At the bulk transition f is zero within errors and develops a value different from zero at the physical transition.

The MC time history of the plaquette is displayed in Fig. 6 (left), and shows a two-phase structure typical of first order phase transitions. The extracted maxima of the plaquette susceptibility ($\propto C_V$) using the reweighted data are shown in Fig. 3. Maxima and their errors are estimated by a simple inspection of the reweighting output. A linear fit of the form $y = a \cdot x + b$ (see Eq. 3.2) gives $a = 0.00079(14) \cdot 10^{-3}$, $b = 0.98(62) \cdot 10^{-3}$, $\chi_{\text{red}}^2 = 1.35$, providing good evidence for a first order phase transition. A fit according to Eq. (3.3) gives $\beta_c(\infty) = 1.3950(4)$.

The Polyakov loop is insensitive to the bulk transition so we used it to detect the position of the physical one, even if, strictly speaking, this quantity is not an order parameter. The Polyakov loop develops an evident double peak structure typical of a first order transition (see Figs. 4,5). In this semilog plot is also clear, by looking at the relative ratio of peaks height and valley height near the transition point, the exponential decreasing of tunneling probability with the volume. In Fig. 6 we show the typical Monte Carlo history of the Polyakov loop. Once again, a clean two-state signal appears. This reflects in a double-peak structure of the observable shown e.g. in Fig. 5. The same FSS analysis as for the specific heat again gives evidence of a first order transition, with a good χ_{red}^2 in the linear fits of peak heights (Figs. 7 and 8). The parameters of the linear fit of the peak heights $y = a \cdot x + b$ are $a = 0.1183(2)$, $b = 60(5)$, $\chi_{\text{red}}^2 = 0.61$. A subtraction of the background is understood. The background is assumed to be weakly dependent on coupling β . This is an educated guess suggested by the zero temperature simulations. The background is estimated by mean of a linear fit of the tails of the peak and being an ultraviolet effect, it is assumed to be the same for all volumes. In practice we took the smallest lattices 6×12^3 , 6×14^3 and some of the extremal points in tails for the fit. The number of points is unessential giving practically the same parameters and a good χ_{red}^2 . The Polyakov loop susceptibility can be also used to determine $\beta_c(\infty)$. Using formula (3.3), we get $\beta_c(\infty) = 1.3951(2)$, which is compatible with the result obtained from the susceptibility of the plaquette.

5. Discussion

As we have stated in the introduction, an asymptotic string tension in G_2 does not exist. Hence, one can question whether this group is confining. This is mostly a semantic problem. In [19] it is argued that because of the absence of the asymptotic string, G_2 gauge theory is not confining. This would fit the idea of confinement as related to centre vortices randomly piercing the Wilson loop. Sharing this view means to accept the logical conclusion that full QCD (in which an asymptotic string tension does not exist because of quark pair production) is not a confining theory. Since it is common understanding that

QCD confines, the essence of confinement must be found in some other property of the theory. In our opinion, this property is a low-energy dynamics dominated by glueballs and mesons (which are colour-singlet states). Colour-singlet states are also present in G_2 at zero temperature. At high temperature the dynamics is instead dominated by a gluon plasma. In this sense, despite the absence of an asymptotic string tension, G_2 gauge theory is a confining theory. Accepting this statement means to infer that centre degrees of freedom are not related to confinement (unless one wants to put all the weight of the centre on the trivial element, see [19]). Hence, the degrees of freedom responsible for colour confinement must be searched for in other properties of the gauge group.

Like $SU(3)$, G_2 is a rank two group, i.e. it has two Cartan generators⁵. It is then an attractive possibility that like in $SU(N)$ pure gauge theories [20, 21, 22] and in full QCD [23, 24] the mechanism for colour confinement is related to the condensation of magnetic monopoles, as it seems to be the case also for the $SO(3)$ gauge theory [25]. An investigation in this direction is currently in progress, and will be reported elsewhere.

6. Conclusions

We studied the thermodynamics of the Yang-Mills theory with gauge group G_2 . The presence of an unphysical transition (most probably due to the choice of the discretised action used in simulations) makes the problem harder. Nevertheless a physical transition is found by looking at plaquette and Polyakov loop susceptibilities. Time histories of the Polyakov group and the plaquette show double peaks typical of first order transitions. A detailed FSS analysis agrees with the first order hypothesis. Hence, we can conclude that G_2 gauge theory has two distinct phases separated by a jump in the free energy. Those phases are immediately identified with the confined (low temperature) and deconfined (high temperature) phase. The same dynamics characterises $SU(N)$ Yang-Mills theories at finite temperature. Since G_2 does not have a (non-trivial) centre, our findings suggest that the dynamics of colour confinement cannot be directly related to the centre of the gauge group, as it has been inferred from previous works on $SU(N)$ gauge theories. At this stage, the possibility that dual superconductivity of the vacuum explains colour confinement is still open. The next step of our study is to investigate the FSS of the monopole creation operator, to test if the dual superconductor picture of confinement works also for G_2 gauge theory.

Acknowledgments

We would thank M. Pepe for various useful discussions on the topic. The work of C.P. has been supported in part by contract DE-AC02-98CH1-886 with the U.S. Department of Energy and B.L. is supported by the Royal Society.

⁵A Cartan generator is a generator which commutes with all the others.

A. G_2 algebra representation

In this appendix we simply report a representation of the 14 generators of the G_2 group [16]. They are normalized such that $\text{tr}(C_i C_j) = -\delta_{ij}$. The first 8 matrices generate the $SU(3) \subset G_2$. Here is also a list of 6 $SU(2)$ subgroups that cover the entire group (useful for the Cabibbo-Marinari update):

1. C_1, C_2, C_3
2. $\sqrt{3}C_8, \sqrt{3}C_9, \sqrt{3}C_{10}$
3. $C_4, C_5, \frac{(C_3 + \sqrt{3}C_8)}{2}$
4. $C_6, C_7, \frac{(C_3 - \sqrt{3}C_8)}{2}$
5. $\frac{(3C_3 - \sqrt{3}C_8)}{2}, \sqrt{3}C_{11}, \sqrt{3}C_{12}$
6. $\frac{(3C_3 + \sqrt{3}C_8)}{2}, \sqrt{3}C_{13}, \sqrt{3}C_{14}$

B. Algebra

$$\begin{aligned}
 C_1 &= \frac{1}{2} \begin{pmatrix} 0 & 0 & 0 & 0 & 0 & 0 & 0 \\ 0 & 0 & 0 & 0 & 0 & 0 & 0 \\ 0 & 0 & 0 & 0 & 0 & 0 & 0 \\ 0 & 0 & 0 & 0 & 0 & -1 & 0 \\ 0 & 0 & 0 & 0 & -1 & 0 & 0 \\ 0 & 0 & 0 & 0 & 1 & 0 & 0 \\ 0 & 0 & 0 & 1 & 0 & 0 & 0 \end{pmatrix} & C_2 &= \frac{1}{2} \begin{pmatrix} 0 & 0 & 0 & 0 & 0 & 0 & 0 \\ 0 & 0 & 0 & 0 & 0 & 0 & 0 \\ 0 & 0 & 0 & 0 & 0 & 0 & 0 \\ 0 & 0 & 0 & 0 & 0 & 1 & 0 \\ 0 & 0 & 0 & 0 & 0 & 0 & -1 \\ 0 & 0 & 0 & -1 & 0 & 0 & 0 \\ 0 & 0 & 0 & 0 & 1 & 0 & 0 \end{pmatrix} \\
 C_3 &= \frac{1}{2} \begin{pmatrix} 0 & 0 & 0 & 0 & 0 & 0 & 0 \\ 0 & 0 & 0 & 0 & 0 & 0 & 0 \\ 0 & 0 & 0 & 0 & 0 & 0 & 0 \\ 0 & 0 & 0 & 0 & -1 & 0 & 0 \\ 0 & 0 & 0 & 1 & 0 & 0 & 0 \\ 0 & 0 & 0 & 0 & 0 & 0 & -1 \\ 0 & 0 & 0 & 0 & 0 & 1 & 0 \end{pmatrix} & C_4 &= \frac{1}{2} \begin{pmatrix} 0 & 0 & 0 & 0 & 0 & 0 & 0 \\ 0 & 0 & 0 & 0 & 0 & 0 & 1 \\ 0 & 0 & 0 & 0 & 0 & 1 & 0 \\ 0 & 0 & 0 & 0 & 0 & 0 & 0 \\ 0 & 0 & 0 & 0 & 0 & 0 & 0 \\ 0 & 0 & -1 & 0 & 0 & 0 & 0 \\ 0 & -1 & 0 & 0 & 0 & 0 & 0 \end{pmatrix} \\
 C_5 &= \frac{1}{2} \begin{pmatrix} 0 & 0 & 0 & 0 & 0 & 0 & 0 \\ 0 & 0 & 0 & 0 & 0 & -1 & 0 \\ 0 & 0 & 0 & 0 & 0 & 0 & 1 \\ 0 & 0 & 0 & 0 & 0 & 0 & 0 \\ 0 & 0 & 0 & 0 & 0 & 0 & 0 \\ 0 & 1 & 0 & 0 & 0 & 0 & 0 \\ 0 & 0 & -1 & 0 & 0 & 0 & 0 \end{pmatrix} & C_6 &= \frac{1}{2} \begin{pmatrix} 0 & 0 & 0 & 0 & 0 & 0 & 0 \\ 0 & 0 & 0 & 0 & 1 & 0 & 0 \\ 0 & 0 & 0 & -1 & 0 & 0 & 0 \\ 0 & 0 & 1 & 0 & 0 & 0 & 0 \\ 0 & -1 & 0 & 0 & 0 & 0 & 0 \\ 0 & 0 & 0 & 0 & 0 & 0 & 0 \\ 0 & 0 & 0 & 0 & 0 & 0 & 0 \end{pmatrix} \\
 C_7 &= \frac{1}{2} \begin{pmatrix} 0 & 0 & 0 & 0 & 0 & 0 & 0 \\ 0 & 0 & 0 & -1 & 0 & 0 & 0 \\ 0 & 0 & 0 & 0 & -1 & 0 & 0 \\ 0 & 1 & 0 & 0 & 0 & 0 & 0 \\ 0 & 0 & 1 & 0 & 0 & 0 & 0 \\ 0 & 0 & 0 & 0 & 0 & 0 & 0 \\ 0 & 0 & 0 & 0 & 0 & 0 & 0 \end{pmatrix} & C_8 &= \frac{1}{2\sqrt{3}} \begin{pmatrix} 0 & 0 & 0 & 0 & 0 & 0 & 0 \\ 0 & 0 & -2 & 0 & 0 & 0 & 0 \\ 0 & 2 & 0 & 0 & 0 & 0 & 0 \\ 0 & 0 & 0 & 0 & 1 & 0 & 0 \\ 0 & 0 & 0 & -1 & 0 & 0 & 0 \\ 0 & 0 & 0 & 0 & 0 & 0 & -1 \\ 0 & 0 & 0 & 0 & 0 & 1 & 0 \end{pmatrix}
 \end{aligned}$$

$$\begin{aligned}
C_9 &= \frac{1}{2\sqrt{3}} \begin{pmatrix} 0 & -2 & 0 & 0 & 0 & 0 & 0 \\ 2 & 0 & 0 & 0 & 0 & 0 & 0 \\ 0 & 0 & 0 & 0 & 0 & 0 & 0 \\ 0 & 0 & 0 & 0 & 0 & 0 & 1 \\ 0 & 0 & 0 & 0 & 0 & -1 & 0 \\ 0 & 0 & 0 & 0 & 1 & 0 & 0 \\ 0 & 0 & 0 & -1 & 0 & 0 & 0 \end{pmatrix} & C_{10} &= \frac{1}{2\sqrt{3}} \begin{pmatrix} 0 & 0 & -2 & 0 & 0 & 0 & 0 \\ 0 & 0 & 0 & 0 & 0 & 0 & 0 \\ 2 & 0 & 0 & 0 & 0 & 0 & 0 \\ 0 & 0 & 0 & 0 & 0 & -1 & 0 \\ 0 & 0 & 0 & 0 & 0 & 0 & -1 \\ 0 & 0 & 0 & 1 & 0 & 0 & 0 \\ 0 & 0 & 0 & 0 & 1 & 0 & 0 \end{pmatrix} \\
C_{11} &= \frac{1}{2\sqrt{3}} \begin{pmatrix} 0 & 0 & 0 & -2 & 0 & 0 & 0 \\ 0 & 0 & 0 & 0 & 0 & 0 & -1 \\ 0 & 0 & 0 & 0 & 0 & 1 & 0 \\ 2 & 0 & 0 & 0 & 0 & 0 & 0 \\ 0 & 0 & 0 & 0 & 0 & 0 & 0 \\ 0 & 0 & -1 & 0 & 0 & 0 & 0 \\ 0 & 1 & 0 & 0 & 0 & 0 & 0 \end{pmatrix} & C_{12} &= \frac{1}{2\sqrt{3}} \begin{pmatrix} 0 & 0 & 0 & 0 & 0 & -2 & 0 & 0 \\ 0 & 0 & 0 & 0 & 0 & 0 & 1 & 0 \\ 0 & 0 & 0 & 0 & 0 & 0 & 0 & 1 \\ 0 & 0 & 0 & 0 & 0 & 0 & 0 & 0 \\ 2 & 0 & 0 & 0 & 0 & 0 & 0 & 0 \\ 0 & -1 & 0 & 0 & 0 & 0 & 0 & 0 \\ 0 & 0 & -1 & 0 & 0 & 0 & 0 & 0 \end{pmatrix} \\
C_{13} &= \frac{1}{2\sqrt{3}} \begin{pmatrix} 0 & 0 & 0 & 0 & 0 & -2 & 0 \\ 0 & 0 & 0 & 0 & -1 & 0 & 0 \\ 0 & 0 & 0 & -1 & 0 & 0 & 0 \\ 0 & 0 & 1 & 0 & 0 & 0 & 0 \\ 0 & 1 & 0 & 0 & 0 & 0 & 0 \\ 2 & 0 & 0 & 0 & 0 & 0 & 0 \\ 0 & 0 & 0 & 0 & 0 & 0 & 0 \end{pmatrix} & C_{14} &= \frac{1}{2\sqrt{3}} \begin{pmatrix} 0 & 0 & 0 & 0 & 0 & 0 & 0 & -2 \\ 0 & 0 & 0 & 1 & 0 & 0 & 0 & 0 \\ 0 & 0 & 0 & 0 & -1 & 0 & 0 & 0 \\ 0 & -1 & 0 & 0 & 0 & 0 & 0 & 0 \\ 0 & 0 & 1 & 0 & 0 & 0 & 0 & 0 \\ 0 & 0 & 0 & 0 & 0 & 0 & 0 & 0 \\ 2 & 0 & 0 & 0 & 0 & 0 & 0 & 0 \end{pmatrix}
\end{aligned}$$

References

- [1] G. 't Hooft, *A planar diagram theory for strong interactions*, *Nucl. Phys.* **B72** (1974) 461.
- [2] C. Borgs and E. Seiler, *Quark deconfinement at high temperature. a rigorous proof*, *Nucl. Phys.* **B215** (1983) 125–135.
- [3] B. Svetitsky and L. G. Yaffe, *Critical behavior at finite temperature confinement transitions*, *Nucl. Phys.* **B210** (1982) 423.
- [4] B. Lucini, M. Teper, and U. Wenger, *The high temperature phase transition in $su(n)$ gauge theories*, *JHEP* **01** (2004) 061, [[hep-lat/0307017](#)].
- [5] J. Liddle and M. Teper, *The deconfining phase transition for $su(n)$ theories in 2+1 dimensions*, *PoS LAT2005* (2006) 188, [[hep-lat/0509082](#)].
- [6] G. 't Hooft, *On the phase transition towards permanent quark confinement*, *Nucl. Phys.* **B138** (1978) 1.
- [7] L. Del Debbio, M. Faber, J. Greensite, and S. Olejnik, *Center dominance and $z(2)$ vortices in $su(2)$ lattice gauge theory*, *Phys. Rev.* **D55** (1997) 2298–2306, [[hep-lat/9610005](#)].
- [8] P. de Forcrand, M. D’Elia, and M. Pepe, *A study of the 't hooft loop in $su(2)$ yang-mills theory*, *Phys. Rev. Lett.* **86** (2001) 1438, [[hep-lat/0007034](#)].
- [9] L. Del Debbio, A. Di Giacomo, and B. Lucini, *Vortices, monopoles and confinement*, *Nucl. Phys.* **B594** (2001) 287–300, [[hep-lat/0006028](#)].
- [10] L. Del Debbio, A. Di Giacomo, and B. Lucini, *Monopoles, vortices and confinement in $su(3)$ gauge theory*, *Phys. Lett.* **B500** (2001) 326–329, [[hep-lat/0011048](#)].

- [11] T. G. Kovacs and E. T. Tomboulis, *Computation of the vortex free energy in $su(2)$ gauge theory*, *Phys. Rev. Lett.* **85** (2000) 704–707, [[hep-lat/0002004](#)].
- [12] A. Barresi, G. Burgio, and M. Muller-Preussker, *Universality, vortices and confinement: Modified $so(3)$ lattice gauge theory at non-zero temperature*, *Phys. Rev.* **D69** (2004) 094503, [[hep-lat/0309010](#)].
- [13] K. Holland, P. Minkowski, M. Pepe, and U. J. Wiese, *Exceptional confinement in $g(2)$ gauge theory*, *Nucl. Phys.* **B668** (2003) 207–236, [[hep-lat/0302023](#)].
- [14] M. Pepe, *Confinement and the center of the gauge group*, *PoS LAT2005* (2006) 017, [[hep-lat/0510013](#)].
- [15] M. Pepe and U. J. Wiese, *Exceptional deconfinement in $g(2)$ gauge theory*, *Nucl. Phys.* **B768** (2007) 21–37, [[hep-lat/0610076](#)].
- [16] S. L. Cacciatori, B. L. Cerchiai, A. Della Vedova, G. Ortenzi, and A. Scotti, *Euler angles for $g(2)$* , *J. Math. Phys.* **46** (2005) 083512, [[hep-th/0503106](#)].
- [17] S. Weinberg, *The quantum theory of fields. vol. 2: Modern applications*, . Cambridge, UK: Univ. Pr. (1996) 489 p.
- [18] W. Janke, *Multicanonical monte carlo simulations*, *Physica A* **254** (1998) 164–178.
- [19] J. Greensite, K. Langfeld, S. Olejnik, H. Reinhardt, and T. Tok, *Color screening, casimir scaling, and domain structure in $g(2)$ and $su(n)$ gauge theories*, *Phys. Rev.* **D75** (2007) 034501, [[hep-lat/0609050](#)].
- [20] A. Di Giacomo, B. Lucini, L. Montesi, and G. Paffuti, *Colour confinement and dual superconductivity of the vacuum. i*, *Phys. Rev.* **D61** (2000) 034503, [[hep-lat/9906024](#)].
- [21] A. Di Giacomo, B. Lucini, L. Montesi, and G. Paffuti, *Colour confinement and dual superconductivity of the vacuum. ii*, *Phys. Rev.* **D61** (2000) 034504, [[hep-lat/9906025](#)].
- [22] J. M. Carmona, M. D’Elia, A. Di Giacomo, B. Lucini, and G. Paffuti, *Color confinement and dual superconductivity of the vacuum. iii*, *Phys. Rev.* **D64** (2001) 114507, [[hep-lat/0103005](#)].
- [23] J. M. Carmona *et al.*, *Color confinement and dual superconductivity in full qcd*, *Phys. Rev.* **D66** (2002) 011503, [[hep-lat/0205025](#)].
- [24] M. D’Elia, A. Di Giacomo, B. Lucini, G. Paffuti, and C. Pica, *Color confinement and dual superconductivity of the vacuum. iv*, *Phys. Rev.* **D71** (2005) 114502, [[hep-lat/0503035](#)].
- [25] A. Barresi, G. Burgio, M. D’Elia, and M. Mueller-Preussker, *A finite temperature investigation of dual superconductivity in the modified $so(3)$ lattice gauge theory*, *Phys. Lett.* **B599** (2004) 278–284, [[hep-lat/0405004](#)].

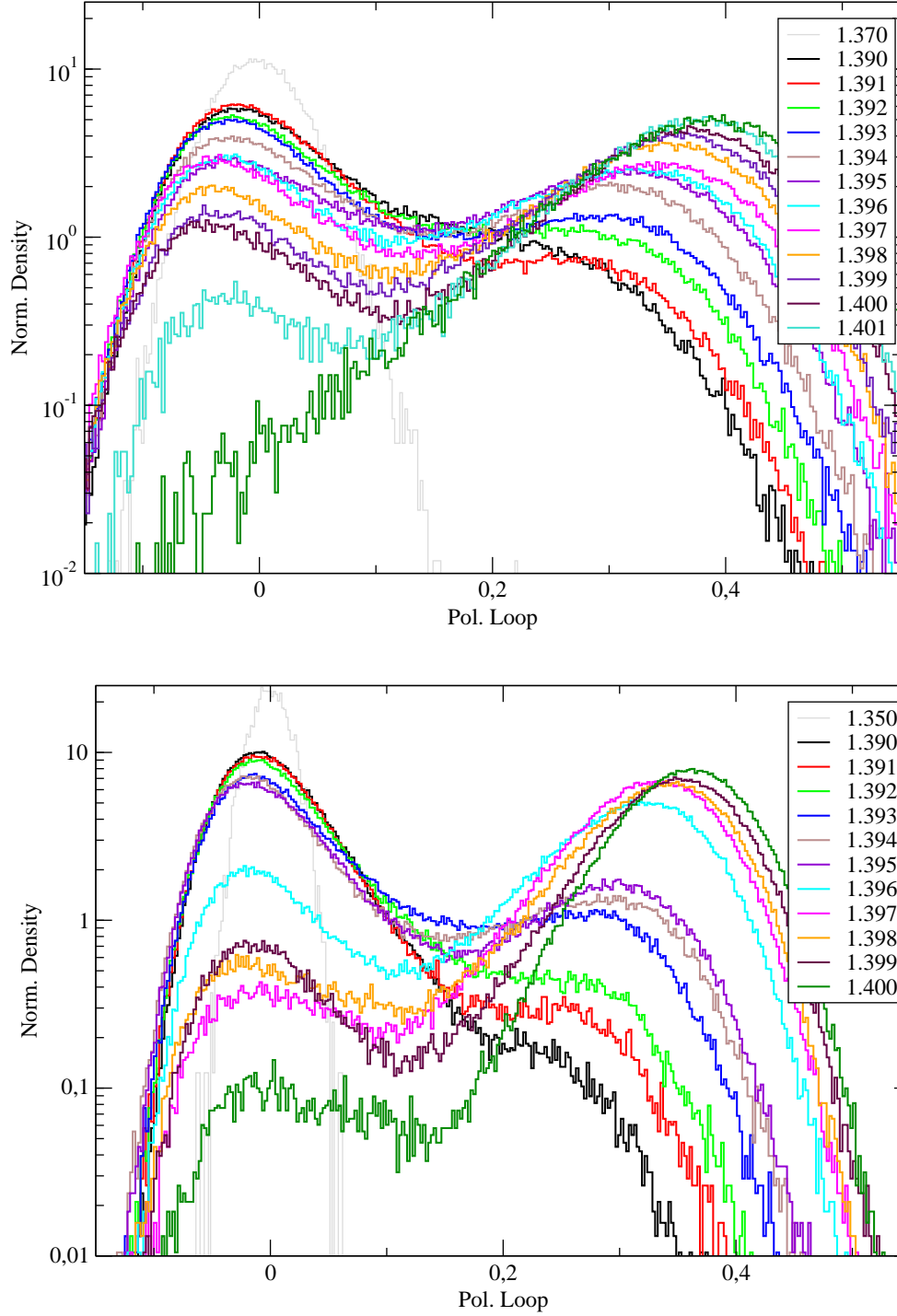


Figure 4: Normalized densities of the Polyakov Loop in a semilog plot for β varying in the range from 1.35, the critical coupling of the bulk transition “ β_{bulk} ”, to 1.401, in the deconfined phase (data from the 6×14^3 lattice for the upper graph and from 6×16^3 for the other - same scales and limits for both axes are used for better comparison). As an aside we notice that far in the confined phase, $\beta_c < 1.395$, the Polyakov loop is zero within errors and this feature can not be explained on the ground of any manifest symmetry of the system. Continues on next page

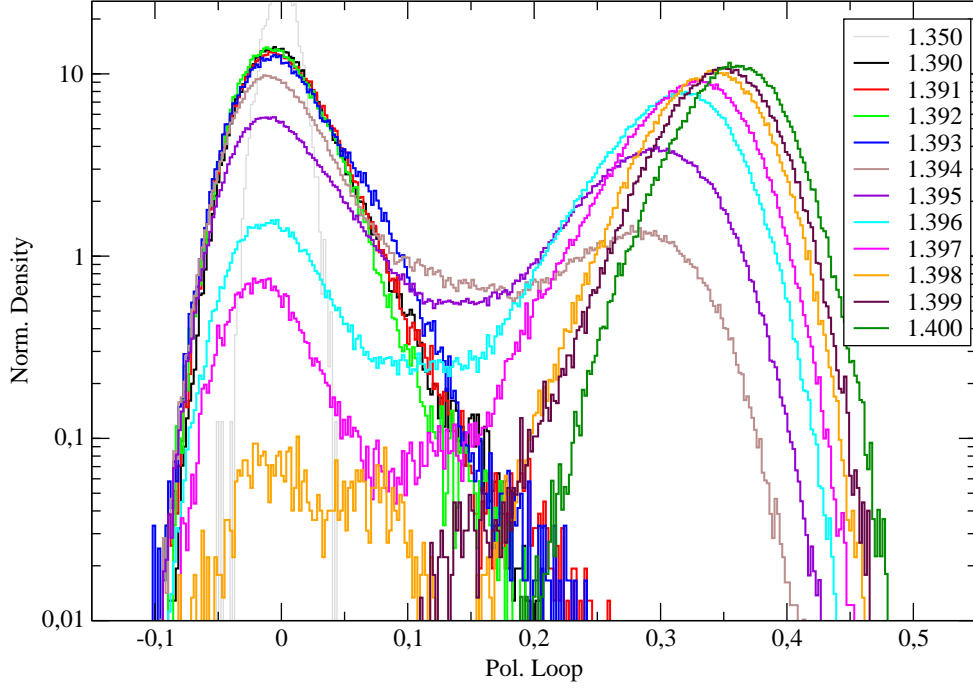


Figure 5: Continues from last page (6×20^3 lattice).

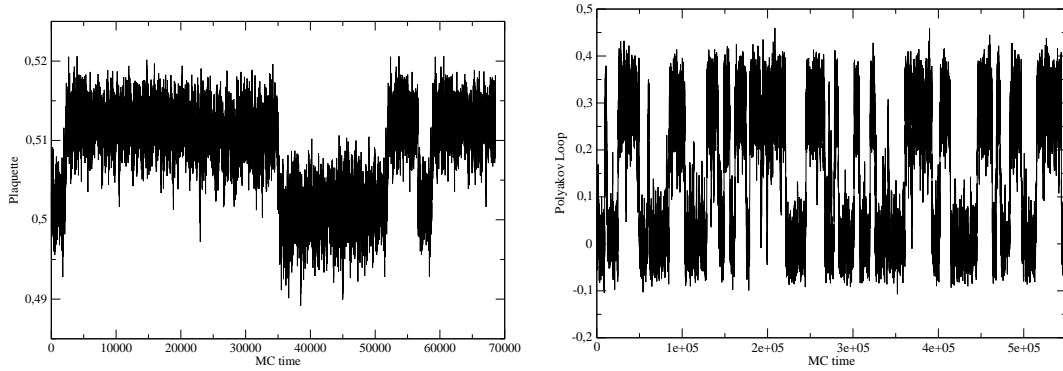


Figure 6: Left: MC history of the plaquette ($\beta = 1.3594, 12^3 \times 4$). Right: A typical Monte Carlo history of the Polyakov loop (data from $\beta = 1.395, 20^3 \times 6$).

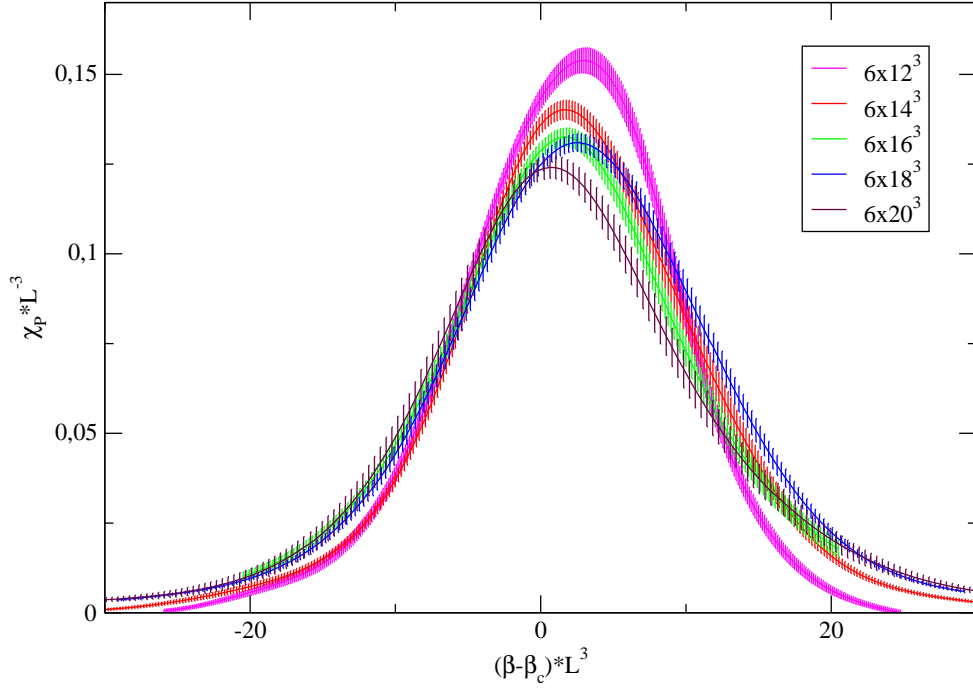


Figure 7: Scaling of the Polyakov loop assuming first order. For the smallest lattice $12^3 \times 6$ corrections to the scaling are evident (even the lattice $14^3 \times 6$ is not big enough but corrections are reduced); $\beta_c = 1.395$ as explained in the text.

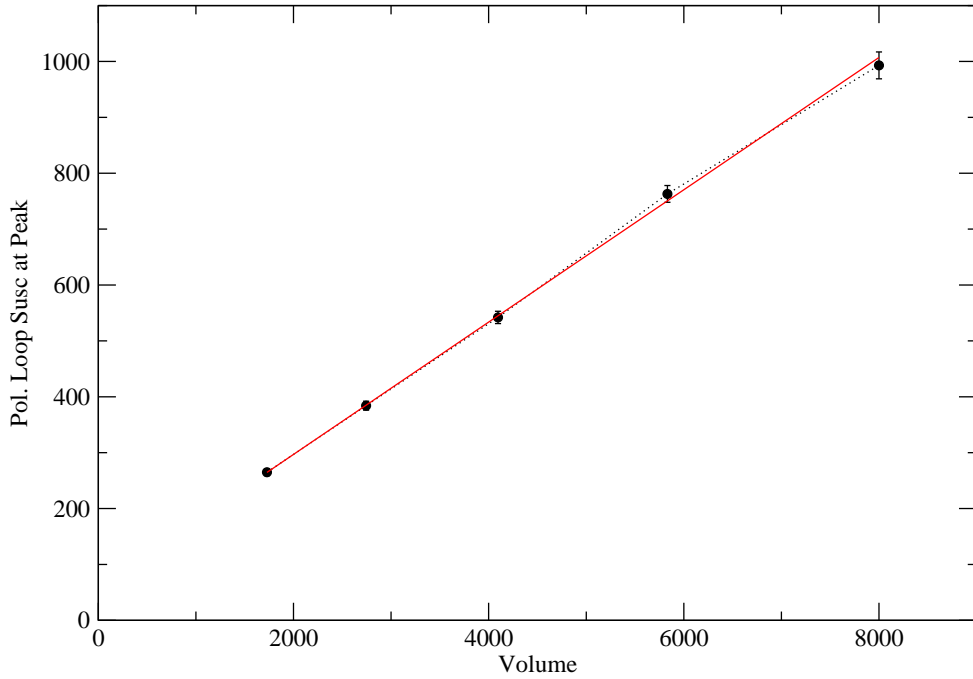


Figure 8: Scaling of the peak of χ_L . The solid line is a linear fit to the data.